

Structure of double row quantum wires in Au/Si(553)

S.K. Ghose ^{a,*}, I.K. Robinson ^a, P.A. Bennett ^b, F.J. Himpsel ^c

^a Department of Physics, University of Illinois, Urbana, IL 61801, USA

^b Department of Physics and Astronomy, Arizona State University, Tempe, AZ 85287, USA

^c Department of Physics, University of Wisconsin, Madison, WI 53706, USA

Received 6 October 2004; accepted for publication 25 February 2005

Available online 17 March 2005

Abstract

We present a new structure for the quantum-wire surface Au/Si(553) obtained from three-dimensional X-ray diffraction measurements. We have found the structure has double row of gold, so the wires are two atoms thick. The diffraction pattern is 1×1 implying a simple (CTR-only) structure, but disorder is necessary in the model to get a good fit, in the form of a 50–50 splitting of the position of one of the gold sites. A 50% occupied Si adatom is also found, which is a common structural theme of Si(111) vicinal surfaces. Since there are insufficient available bonds for an adatom to reside in every unit cell, the Au splitting can be seen as a consequence of the alternating presence of the adatoms. No half order diffraction was observed, so any local order of these features must be assumed to be short-range.

© 2005 Elsevier B.V. All rights reserved.

Keywords: X-ray diffraction; Vicinal single crystal surfaces; Faceting; Self-assembly; Surface structure; Gold; Silicon

1. Introduction

The study of artificial nanostructures is fueled both by their unusual physical properties and by their potential use in ultrasmall electronic devices. One approach to the fabrication of such structures is self-assembly, which can produce features smaller than those possible by conventional lithographic techniques. This paper focuses on a particular form of self assembly process that pro-

duces linear structures with well defined number of atomic rows per period on vicinal Si(111) surfaces.

On flat Si(111), the deposition of gold leads to anisotropic 5×2 reconstructions [1–4]. Similar $n \times 1$ and $n \times 2$ reconstructions are formed by deposition of silver [5], alkali metals [6,7], alkaline earths [6,7] and rare earths [8]. However, for flat surfaces the length of the chains is limited due to domain structure imposed by three fold symmetry of the underlying lattice, which allows three equivalent chain directions ($[1, -1, 0]$, $[0, 1, -1]$, $[-1, 0, 1]$). Stepped silicon surfaces break the

* Corresponding author. Tel./fax: +1 6302520433.

E-mail address: ghose@mrl.uiuc.edu (S.K. Ghose).

threefold symmetry of the substrate and lead to a single domain along the step edge in one of the three equivalent chain directions. Low coverage of gold on a flat Si(111) surface gives a stable 5×1 or 5×2 structure which consists of two Au rows per unit cell [2,9,10]. The 5×2 is complicated by considerable disorder, but appears to involve substitution of rows of Au atoms into the surface layers at low symmetry sites combined with Si adatoms [2]. In the same way at low coverages there is only a single gold chain on the terrace of such vicinal surfaces [11–13], while high coverage flat Si(111) 5×2 -Au structure consists of two Au rows per unit cell [14,10].

Vicinal Si(111) surfaces containing stable $[1, -1, 0]$ steps can be classified into two groups, one with its normal tilted towards the $[1, 1, -2]$ azimuth with one broken (dangling) bond and the other towards $[-1, -1, 2]$ with two broken bonds at the step edge atom. Si(557) and Si(553) surfaces are examples from these two groups of vicinal surfaces [11]. The Si(553) stepped surface consists of $4\frac{1}{3}$ rows wide Si(111) terraces having a single dangling bond at the step edge. It has been reported from STM measurements and total energy calculations [13], that Au/Si(553) surface has a single row of Au substituting for one of the terrace Si atoms. The structures of gold on vicinal Si surfaces are all very sensitive to preparation conditions and precise coverage [15]. Total energy calculations are useful to validate the structure of such systems, but always require a knowledge of the complete structure at the full atomic level in 3D. STM is strongly influenced by electronic structure as well as physical structure. For definitive atomic structure determination, a method sensitive to the locations of the atomic cores, such as surface X-ray diffraction (SXRD) is preferable.

We report here, using surface X-ray diffraction, that the structure of Au on Si(553) has two chains of Au per surface step. It is a structure with 2 gold atoms in the unit cell decorating the step edge, so forming “nanowires”. The Au atom in one chain is near the step edge Si atom and the outer Au chain is split into two 50%-occupied sites, one displaced upwards and the other down. There is a 50%-occupied Si directly underneath the outer Au row, with adatom like coordination. The upper

site of the Au is found to correlate with the presence of the adatom, as if forming a 1×2 structure, although no such long-range order was detected in the diffraction.

2. Experimental procedure

Our experiments were performed on beamline X16A of the National Synchrotron Light Source (NSLS) at Brookhaven National Laboratory, which is customized for high-resolution diffraction experiments in ultrahigh vacuum (UHV) [16]. The beamline uses a bent cylindrical mirror to focus bending magnet radiation into 1 mm^2 at the sample. The incident beam was monochromatized by parallel Si(111) crystals. The diffracted beam was detected by a position sensitive detector (PSD) oriented along the surface normal behind $2 \times 20 \text{ mm}^2$ slits placed 0.6 m away.

The sample was aligned by means of bulk Bragg reflections. The bulk Bragg reflections reindexed according to the surface unit cell [17] chosen to be orthorhombic with axes lying parallel and perpendicular to the surface so that all diffraction appears at integer h and k . For example, the cubic $(1, 1, -1)$ bulk reflection indexes as $(8, 0, 7)$, while the $(2, 2, 0)$ bulk reflection indexes as $(6, 0, 20)$. Reciprocal space indices transform according to the following matrix equation,

$$\begin{pmatrix} h \\ k \\ L \end{pmatrix}_S = \frac{1}{2} \begin{pmatrix} 3 & 3 & -10 \\ -1 & 1 & 0 \\ 10 & 10 & 6 \end{pmatrix} \begin{pmatrix} h \\ k \\ l \end{pmatrix}_B \quad (1)$$

where “S” and “B” denote surface and bulk, respectively. Using this coordinate system, all diffraction from the simple termination of Si(553) surface (with uniformly spaced steps) lies along rods with integer in-plane indices, h and k , indicating a 1×1 structure. All rods intersect bulk Bragg peaks every 59 units along L , except where forbidden by diamond-lattice selection rules. This identifies them all to be crystal truncation rods (CTRs) [18].

Our samples were made from a wafer cut at an angle of 14.4° from $[1, 1, 1]$ towards $[1, 1, -2]$, which makes it close to the Si(13, 13, 7) orientation.

Samples were prepared in ultrahigh vacuum (10^{-10} Torr range) by electrical heating of wafers to 1200 °C for flash cleaning followed by brief annealing at 850 °C. Scans along $(h, 0, 11)$, parallel to the surface, were then taken to verify the orientation of the surface facets by measuring their angle to one of the nearby bulk $\{111\}$ reflections, indexing at $\text{Si}(8, 0, 7)$. The clean surface did not have any reconstructions apparent: the h scan cutting through the CTRs, shown in Fig. 1, shows peaks at equally spaced h values which confirms the 1×1 state. The peak intensity was low because of the small contribution of Si atoms to the CTR scattering.

Gold was then evaporated from a coated tungsten filament onto the sample held at 650 °C at a

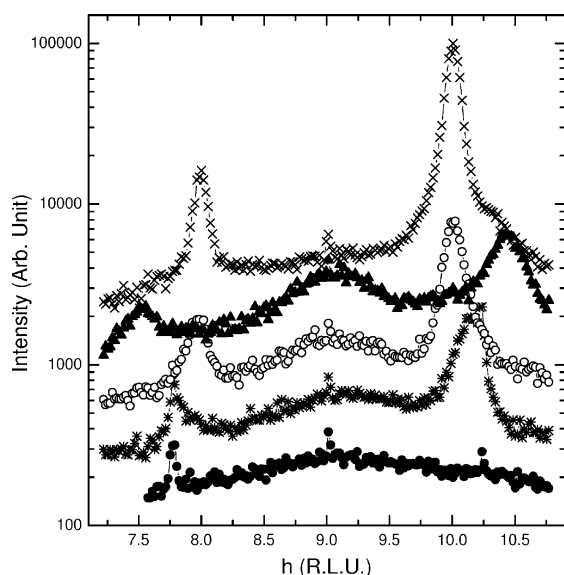


Fig. 1. Intensity measured parallel to the surface along the h -direction of the reciprocal lattice along $(h, 0, 11)$, some distance above the bulk Bragg peak at $(8, 0, 7)$. The peaks move with dose as the facet orientation changes and only appear at integers for the (553) orientation used for indexing. Solid circles are for the clean sample before deposition. The peak positions indicate a $(13, 13, 7)$ facet orientation. Stars are after 0.27 ML where the $\text{Si}(995)$ facets are displayed. Open circles are after 0.54 ML where the $\text{Si}(553)$ facets are displayed. Upright triangles (0.81 ML) do not correspond to a simple orientation and show a poorly ordered surface. The crosses were measured for the final preparation of the surface with a dose of 0.45 ML. The curves are offset by factors of 2 on the logarithmic scale for clarity.

deposition rate of 0.09 ML/min. Here 1 ML (monolayer) is defined as one Au atom per surface Si atom on $\text{Si}(111)$ that corresponds to 7.83×10^{14} atoms/cm². The coverage was determined from the calibration curve obtained from the measurement of deposition time and thickness (quartz balance) needed to form $\sqrt{3} \times \sqrt{3}$ structure of $\text{Au}/\text{Si}(111)$. After calibrating the coverage on a flat $\text{Si}(111)$ sample, we made further tuning of the Au coverage on the vicinal $\text{Si}(111)$ surface. We observed different facets on the same sample as the coverage of Au was increased. In Fig. 1 we show the measured structure factors for different coverages, scanned along the same $(h, 0, 11)$ direction of the reciprocal lattice. Converting the spacing of the peak positions to an angle using the required trigonometry, we found the orientations of the different faceted surfaces with respect to $[1, 1, 1]$ axis. In Fig. 1, we observed the clean surface was oriented towards $\text{Si}(13, 13, 7)$ surface. At a coverage of 0.27 ML we observed the surface faceted to $\text{Si}(995)$. The (553) orientation was observed at a coverage of 0.54 ML. At a coverage of 0.81 ML the surface becomes multifaceted as the peaks become broader. Finally we prepared a $\text{Si}(553)$ -Au surface on a freshly cleaned sample with this pre-estimated coverage followed by brief annealing at 830 °C. This final coverage corresponds to 2.0 Au atoms per $\text{Si}(553)$ surface unit cell. We note that earlier experiments on $\text{Si}(553)$ -Au had estimated a coverage of only one Au atom per $\text{Si}(553)$ unit cell [13]. Our surface had a well ordered 1×1 structure with no reconstruction. We did not see evidence of any other facet in our h -scan, so presumed it is too small to be observed. In Fig. 1 we show the h -scan of the final well-ordered Au-Si(553) surface that was used for the crystallographic measurements.

About 850 equivalent intensities were measured, spanning the 3D reciprocal space. To extract the structure factors quantitatively, the intensities were integrated over orientation angle ϕ , background subtracted and corrected for the Lorentz factor, polarization and active sample area [18]. The structure factors were averaged assuming pm symmetry to yield 450 independent measurement points, positioned along 24 crystallographically

distinct CTRs, with a reproducibility of 5.4% [19].

3. Results

A striking feature about the CTRs measurements is that there is a small variation (about 20%) in the structure factors with L in all the rods, except in the vicinity of Bragg peaks, where they necessarily diverge. This is because Au dominates the scattering for all L values except at Bragg positions. This small modulation of the CTR informs us there must be more than one Au atom present in the unit cell, unlike the CTRs measured for the case of Au/Si(557) [12]. This information is important to model the structure correctly.

The crystallographic tool most suitable to analyze these measurements in a model-independent way is the Patterson (pair correlation) function [19]. The Fourier transform of the structure factors gives the Patterson function map directly. A positive peak on the map means that pairs of atoms in the structure are separated by a particular vector. By interpreting these vectors in the map, it is possible to suggest a model for the proper structure to test the measured data further. We have carefully adjusted the number of data points close to the bulk Bragg points that are included in the Patterson map so as to get the clearest picture of the surface. We have also removed the Patterson origin peak in the standard way [20]. In our case the Patterson map is more complicated than the simple case of one heavy atom per unit cell for Au/Si(557) [12].

Fourier transformation of our measurements gives the Patterson map shown in Fig. 2. Each heavy Au atom produces an image of the structure and its inverted twin image appearing in the map. Considering this map to be a superposition of the positive (x, z) and negative $(-x, -z)$ Si positions with respect to Au at the origin, the map suggests there is a gold (Au-1) atom present at one of the bulk Si sites. The bulk Si peaks which are distinctly visible, correspond to Au-1–Si vectors. The presence of additional intense peaks, “A” and “B”, at sites that do not fall on the Si lattice (Fig. 2), inform us about the location of the second heavy

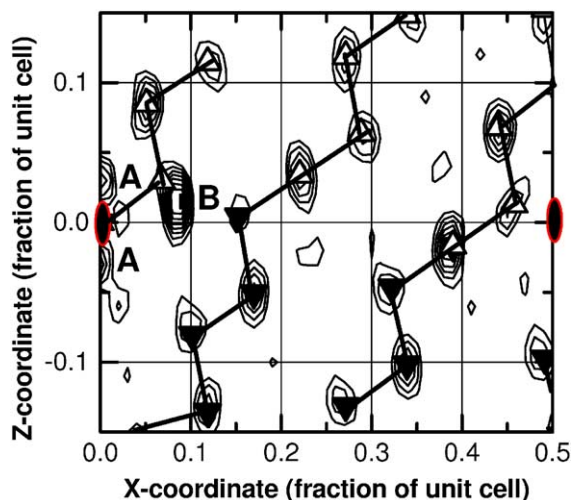


Fig. 2. Positive contours of the $y = 0$ section of the Patterson (pair correlation) function obtained directly by Fourier transformation of the CTR intensities observed for Au/Si(553). The map has twofold rotational symmetry about the origin ($x = 0, z = 0$) (peak suppressed), and about the center ($x = \frac{1}{2}, z = 0$) as shown by diad symbol. Because the unit cell is centered, the $y = \frac{1}{2}$ section can be obtained by a shift of $\frac{1}{2}$ in x . Labels “A” and “B” indicate additional peaks not appearing in the bulk Si lattice (solid and open triangles). The interpretation drawn from these peaks is described in Fig. 3.

atom. The additional peaks in the Patterson are interpreted as the vectors between the heavy atoms positions within the unit cell, illustrated in Fig. 3. The elongation of the peak “B” (Fig. 3b) identifies two vectors that could reasonably explain vectors “1” and “2” in Fig. 3a between the Au-1 and Au-2 atoms. This elongation suggests two z positions of the second Au atom (Au-2 and Au-3). The peaks “A” directly above and below the origin (Fig. 3b) are identified as a third vector “3” between the two positions, Au-2 and Au-3 in Fig. 3a. The intensity enhancement of the alternate bulk Si peaks in the Patterson can be explained by the multiple Au-atom–Si vectors. While the Patterson map (Fig. 2) supports the idea of three Au atoms per unit cell, two of them fall unrealistically close together. The Patterson map guides us to suggest specific atomic models, which can then be tested directly from the measured structure factors.

Fitting of experimental data with a model for bulk terminated Si(553) surface structure without

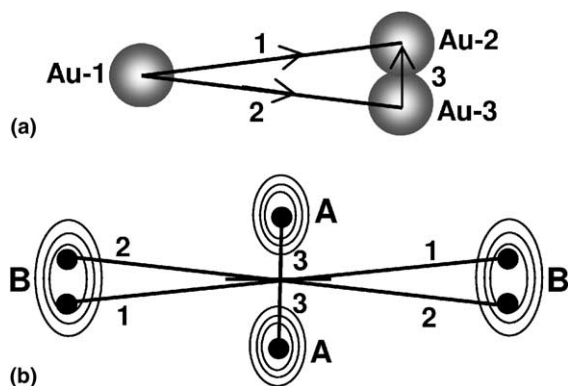


Fig. 3. Interpretation of the atomic positions for Au atoms drawn from the Patterson map (Fig. 2). (a) Position of the three Au atoms, Labeled as Au-1, Au-2 and Au-3, shown in the same view as Fig. 2. Vectors “1” and “2” define the vectors between Au-1 and the two split Au atom positions Au-2 and Au-3, respectively. Vector “3” defines the vector between Au-2 and Au-3. (b) Six peaks obtained in the Patterson map are generated by the three atoms. Peak “B” is elongated due to merging of the two peaks generated by vectors “1” and “2”.

Au gave a χ^2 value of 80. Therefore we needed a model with the presence of Au on the Si(553) surface. We considered the model suggested by Crain et al. [13], with one Au substituting for one Si at the middle of the terrace. The model was tested using the ROD program [21] with 35 free positional parameters, variable occupancy for Au and Debye–Waller factors for the atoms at the top layer and Au. This model did not give a good fit, with $\chi^2 = 20$. We also tested different models by positioning a single Au atom at different Si substitution sites, assuming a simple structure, but none of the models improved the fit.

Following the structure supported by Patterson map (Fig. 3a) we formulate the model by considering three Au atoms (Au-1, Au-2 and Au-3) on the surface. By merging Au-2 and Au-3 into a single combined atom, we first determined the position of the Au atoms within the unit cell, moving them as a pair separated by the distance between origin and peak “B”, read off the Patterson map. We found that both Au atoms decorate the step edge rather than replacing Si at the center of the terrace. This brings down the χ^2 to 8. All other positions of the pair gave $\chi^2 > 8$. This position of Au atoms leaves a big gap below Au-2, so

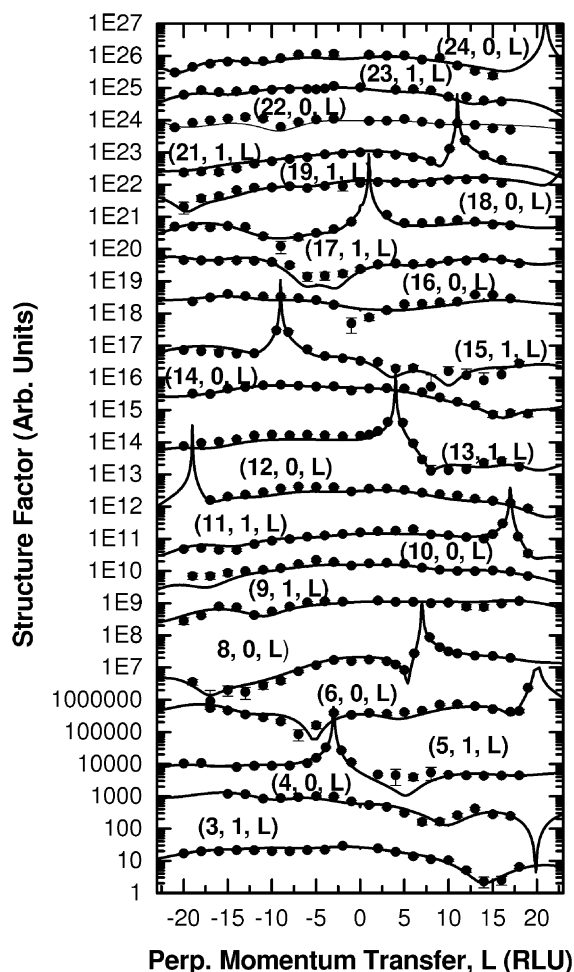


Fig. 4. Measured X-ray structure factors for CTRs of Au/Si(553) surface together with the calculated curves from the best fit model. The curves are offset by factors of 10 on the logarithmic scale. Solid circles represent the measured data and solid line represents the fit.

we then tested the structure by inserting Si atoms below the Au-2 atom, at variety of sites. The one that gave the best fit is the site with “adatom” like bonding to the Si terrace. Now again refining parameters of the two gold atoms and Si adatom, we obtained a reasonable fit. The Si adatom site turned out to be 50%-occupied. To accommodate the third Au in the Patterson map it was found that the Au-2 atom fits better if it is split into two 50%-occupied sites, one *up*, one *down*. The fitted separation of Au-2 and Au-3 is $0.6 \pm 0.2 \text{ \AA}$,

consistent with the Patterson. With all these additional features we brought down the χ^2 value to 7. This relatively large value of χ^2 is acceptable because the χ^2 value depends on systematic error [19] which were probably underestimated while averaging the structure factors with pm symmetry. Errors of 10% are more usual for this instrument, which would reduce the χ^2 by a factor of 4. So we take this as the final fit. The final structure is shown in Fig. 5a and b.

We emphasize that the evidence for a three Au atom structure comes directly from the data, via its Fourier transform, the Patterson. Several extra peaks appear near the origin that can not be explained as Au–Si vectors. This is in stark contrast to Au/Si(557) where the origin region of the Patterson is clear. An additional effect of the multi-Au structure is that the Au–Si peaks in the Patterson (far from the origin) alternate in brightness.

The apparent doubling of the period in the y direction, indicated by the partial occupancies at two sites, raises the question of whether these are correlated. Correlations were checked by constructing a 1×2 model with Au-2, Au-3 and just one Si adatom as shown in Fig. 5c. Since there were no half order peaks present in the measurement, we tested this model by reindexing the integer-order data accordingly. The version of the model with Au-2 above the adatom and Au-3 where there is no adatom gave a χ^2 value of 6.5 while the reverse gave a worse χ^2 value of 7.2. Thus the 50% Au-2 is confirmed to lie above the 50% adatom.

The Au-1 atom sits at a reasonable bonding distance of $2.41 \pm 0.2 \text{ \AA}$ from the edge Si atom. This gold atom is aligned along the step edge. The geometry in Fig. 5b is reasonable for a Si surface. All surface layer Si atoms were relaxed during the

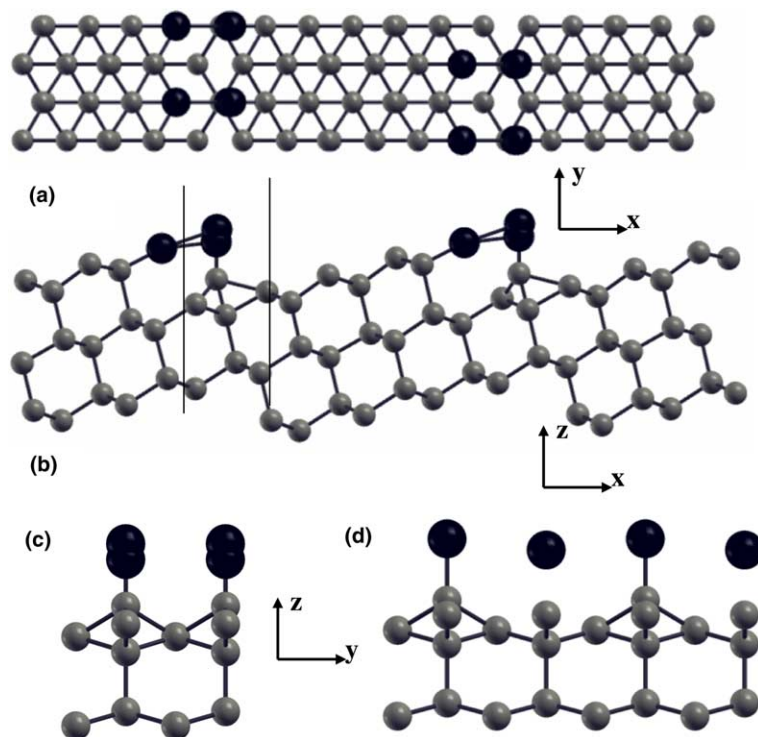


Fig. 5. Final structural models of the Au/Si(553) surface after refinement of the atomic positions. The atoms are drawn as balls with grey colors for Si atoms and black colors for Au atoms. (a) Top (xy) view. (b) Side (xz) view of the model showing the Au atoms at the edge of the steps. (c) Side (yz) view of the model in single unit cell along y . (d) yz view of the inferred 1×2 model with preferred assignment of Au-2 and Au-3. Two vertical lines in (b) denote the section that is cut out for the yz view.

fit, but the displacement of the surface Si layers were found to be very small. The average bond lengths for all the Si–Si bonds (except adatoms) were found to be 2.38 \AA with a standard deviation of 0.06 \AA . The bulk bond length is 2.35 \AA . The adatom geometry showed a backbond length of $1.98 \pm 0.2 \text{ \AA}$, the poor reliability coming from the low occupancy. The occupancies for Au-1 atom are found to be 70% and those of Au-2 and Au-3 are 38% each. The total occupancy of Au atoms gives an observed coverage of 1.46. This value of Au occupancy does not match to the deposition calibration of 2.0 Au atom per unit cell; this is believed to arise from incomplete coverage or disorder in the structure.

The Au/Si(553) structure is therefore a double Au-row structure with latent 1×2 ordering. The refined co-ordinates of the final model are shown in Fig. 5. Since no half order peaks were seen, the inferred 1×2 ordering must be short range, extending less than about 20 unit cells. In Fig. 4 we have shown the best fit curves for this model along with the experimental data, showing a good agreement.

4. Discussion

An unreconstructed Si(111) 1×1 terrace requires three upper bilayer dangling bonds to attach an adatom. Hence adatoms can only attach to every second surface Si along y . It requires a doubled 1×2 unit cell, doubled along y direction repeating the bulk Si structure, for there to accommodate (100% occupied) adatoms. The observation of a 50% occupied adatom in a unit cell with single repeat of the bulk structure in y direction inherently signifies a 1×2 structure. Similar to the Au/Si(557) structure [12] the implication is that the unit cell is doubled in the y -direction along the step edge forming a 1×2 structure. In their STM studies [22] of Au on vicinal Si(111) surface, Shibata et al. showed adatom like protrusions are spaced every two unit cells. In our model, the alternating adatom is the same as in the 557 [12] and (111)-vicinal structure [22].

The gold atom in the second row is having two split sites, Au-2 and Au-3, with 50% occupancy.

The Au-2 site lies above the Si adatom at a distance of $2.37 \pm 0.1 \text{ \AA}$. The bond length of Au-3 to Si adatom is $1.8 \pm 0.2 \text{ \AA}$ and separated from Au-2 by $0.6 \pm 0.2 \text{ \AA}$. It is not possible for atoms to be as close together as the latter distance, which supports the notion that Au-2 and the adatom are alternating in a superstructure. The Au-3 site lies within a pocket made by Si atoms without any close contacts with the underlying Si.

As mentioned above, Si(557) is a vicinal surface in which the edge atoms have double dangling bonds. During relaxation of the surface, these double dangling bonds gets saturated through rebonding [12,23] creating additional Si–Si bonds. In case of Si(553) surface, there is a single broken bond at the step edge. The most favorable way to saturate single bonds could be through covalent bonding instead of rebonding. In our case the Au-1 atom appears to get attached to the edge Si atom through a covalent type of bonding. The bond length of 2.41 \AA also supports the bonding configuration for covalent Au–Si bonding.

5. Conclusions

A model has been presented here for the quantum-wire surface structure of Au/Si(553). The structure contains a double row of gold, so the wires are two atoms thick. The measured X-ray diffraction pattern is 1×1 with all data falling along Crystal Truncation Rods (CTRs). Disorder is found to be necessary in the form of a 50% occupied Si site with adatom-like bonding and also in 50–50 splitting of the position of the adjacent gold site. The adatom can be understood to be a common structural theme of Si(111) vicinal surfaces. Since there are insufficient available bonds to fill every unit cell, the Au splitting can be seen as a consequence of the alternating presence of the adatoms. We have not observed any half order peaks to confirm the long range order of the 1×2 model. Hence the 1×2 ordering might extend over only short range.

In summary, we have analyzed the structure of a Au/Si(553) prepared by calibrated dosing from a more steeply misoriented surface. The dose was

optimized to obtain the strongest peaks of the (553) facet direction and corresponded to a coverage of 2.0 Au atoms per 1×1 unit cell. This is twice as large as the coverage used in previous STM and photoemission studies [13], which indicates that there are probably two different structures, one containing a single Au chain per unit cell, the other two. Our analysis is definitive about the following features of the structure: (i) two Au atoms, not one, appear in the 1×1 surface unit cell; (ii) the registry of the Au atom pair with respect to the Si places one of them close to a bulk Si site in the upper half plane of the double layer; (iii) there is a vertical splitting of the position of the second of the two Au sites. Based on this information, we have composed a complete model of the surface including all Si atoms, but the data is less sensitive to Si than to Au. This final model locates a 50% occupied Si ‘adatom’ underneath the second Au, which fills the gap that would otherwise exist there. This adatom is correlated with the splitting, suggesting a local doubling of the unit cell. It is hoped that the structural information obtained here will help inspire theoretical calculations to confirm the various features of the structure by first-principle total-energy calculations.

Acknowledgement

We acknowledge J.N. Crain for advice about the surface preparation and helpful discussions. This work is supported by Air Force Office of Scientific Research MURI grant F49620-01-1-0336. The X16A beam line is supported by the DOE under DEFG02-91ER45439 and NSLS is supported by DOE under DEAC02-98CH10886.

References

- [1] R. Feidenhansl et al., in: M.G. Lagally (Ed.), *Ordering and Growth at Surfaces*, Plenum Press, New York, 1990.
- [2] D. Grozea, E. Bengu, L.D. Marks, *Surf. Sci.* 461 (1997) 23, and references therein.
- [3] K.N. Altmann et al., *Phys. Rev. B* 64 (2001) 035406.
- [4] R. Losio, K.N. Altmann, F.J. Himpsel, *Phys. Rev. Lett.* 85 (2000) 808.
- [5] J. Kuntze, A. Mugara, J.E. Ortega, *Appl. Phys. Lett.* 81 (2002) 2463.
- [6] S.C. Erwin, H.H. Weitering, *Phys. Rev. Lett.* 81 (1998) 2296.
- [7] D.Y. Petrovykh, K.N. Altmann, J.-L. Lin, F.J. Himpsel, F.M. Leibsle, *Surf. Sci.* 512 (2002) 269.
- [8] A. Kirakosian, J.L. McChesney, R. Bennewitz, J.N. Crain, J.-L. Lin, F.J. Himpsel, *Surf. Sci.* 498 (2002) L109.
- [9] A.A. Baski, J. Nogami, C.F. Quate, *Phys. Rev. B.* 41 (1990) 10247.
- [10] E. Bauer, *Surf. Sci.* 250 (1991) L379.
- [11] J.N. Crain, J.L. McChesney, F. Zheng, M. Gallagher, P.C. Snijders, M. Bissen, C. Gundelach, S.C. Erwin, F.J. Himpsel, *Phys. Rev. B* 69 (2004) 125401.
- [12] I.K. Robinson, P.A. Bennett, F.J. Himpsel, *Phys. Rev. Lett.* 88 (2002) 96104.
- [13] J.N. Crain, A. Kirakosian, K.N. Altmann, C. Bromberger, S.C. Erwin, J.L. McChesney, J.-L. Lin, F.J. Himpsel, *Phys. Rev. Lett.* 90 (2003) 176805.
- [14] S.C. Erwin, *Phys. Rev. Lett.* 91 (2003) 206101.
- [15] W. Swiech, E. Baur, M. Munschau, *Surf. Sci.* 253 (1991) 283.
- [16] P.H. Fuoss, I.K. Robinson, *Nucl. Instrum. Meth.* 222 (1984) 171.
- [17] I.K. Robinson, D.J. Tweet, *Rep. Prog. Phys.* 55 (1992) 599.
- [18] I.K. Robinson, *Phys. Rev. B* 33 (1986) 3830.
- [19] I.K. Robinson, D.E. Moncton, G.S. Brown, *Handbook of Synchrotron Radiation*, vol. 3, North-Holland, Amsterdam, 1986.
- [20] G.H. Stout, L.H. Jensen, *X-ray Structure Determination, a Practical Guide*, second ed., John Wiley Sons, 1989.
- [21] E. Vlieg, *J. Appl. Cryst.* 33 (2000) 402.
- [22] M. Shibata, I. Sumita, M. Nakajima, *Phys. Rev. B* 57 (1998) 1626.
- [23] D. Sanchez-Portal, J.D. Gale, A. Garcia, R.M. Martin, *Phys. Rev. B* 65 (2002) 81401.